#6786

F. Haghighat

Z. Jiang

J. C. Y. Wang

Centre for Building Studies,
Concordia University,
Montreal, Quebec H3G 1M8

F. Allard

Centre de Thermique de l'INSA de Lyon,
URA CNRS 1372,
INSA bat. 307
F. 69621 Villeurbanne Cedex,
France

Air Movement in Buildings Using Computational Fluid Dynamics

This paper presents the development of a three-dimensional numerical model to study the distributions of indoor air velocity, air temperature, contaminant concentration, and ventilation effectiveness in a two-zone enclosure. The numerical model is based on the $k-\epsilon$ two-equation model of turbulence and the SIMPLE algorithm. The false-time step and ADI iteration procedure are employed. The results of the computed velocity and temperature profiles and convective heat transfer by the model are in good agreement with the measurements as well as with the prediction of the PHOENICS code.

Introduction

Health, comfort, and energy conservation are important parameters to consider in relation to the design of a building. Designers of buildings and HVAC systems require the tools to evaluate the parameters regarding air flow in buildings with the end results being better indoor air quality, thermal comfort, as well as increased confidence in the performance of buildings, and the system optimized for low-energy consumption.

The processes of air and contaminant flow through a building are three-dimensional and occur under complex conditions. These processes can be described by a set of conservation equations; namely the continuity, momentum, and energy equations with appropriate boundary conditions. Since these nonlinear, second-order partial differential equations are coupled with one another, an exact solution has not yet been obtained. Therefore, analytical study has to be based either on very rough and simplified models in which the distributions of properties are considered to be uniform, or on numerical methods. Experimental measurement and numerical simulation are usually used to investigate the intra and interzone convective heat and mass transfer in buildings. However, the air movement in a multizone enclosure is affected by many parameters, such as the dimension of the enclosure, the size and the location of the door opening, the locations of the ventilation inlet and outlet, the temperature conditions of walls, etc. It is difficult to deal with the variations in parameters in an experimental study.

Computational fluid dynamics has the advantage of studying the convective heat and mass transfer within and between zones. A validated numerical model not only allows a research effort to be carried over a short period of time and at less expense to cover a wide range of boundary conditions encountered in buildings, but also provides an overall view on the field distributions of all of the important factors. A number of works have been done in this area (Whittle, 1986). The majority of the cases dealt with single enclosures.

Natural convection in an enclosed cavity has been investigated by many researchers (i.e., Catton, 1978; Ostrach, 1982; Markatos and Pericleous, 1984; Lin and Nansteel, 1987; Hadjisophocleous et al., 1988; Gadgil et al., 1984). Markatos and Pericleous (1984) studied natural convection in an enclosure with both laminar and turbulent flows. With the two-dimensional approximation, the classical boundary conditions for natural convection were used: The two side walls were at constant but different isothermal temperatures while the floor and ceiling were insulated. The SIMPLEST algorithm was adopted to solve the finite difference equations. Solutions were computed for Ra from 10^3 to 10^{16}. The criterion for switching from laminar flow to turbulent flow used in their study was the Rayleigh number at 10^6.

Lemarie (1987) applied the CHAMPHxN computer code (Pun and Spalding, 1976) coupled with a radiation model to compute the air movement and heat transfer in a room heated by a radiator.

The PHOENICS code has been used for two or three-dimensional analysis of convective heat and mass transfer in buildings by a number of researchers (i.e., Holmes, 1982; Markatos, 1983; Jones and Sullivan, 1985; Chen and Van der Kooi, 1988). Markatos and Cox (1984) applied the modified PHOENICS to predict the development of a fire and the contaminant concentration distribution within a shopping mall. The fire was simulated by heat and contaminant sources. Both steady and transient cases were predicted, either for a fixed heat release rate or for a linearly growing fire reaching the fixed rate at three minutes from ignition.

Berne and Villand (1987) described the three-dimensional thermohydraulic code TRIO-VF which can handle laminar or

Contributed by the Solar Energy Division of THE AMERICAN SOCIETY OF MECHANICAL ENGINEERS for publication in the JOURNAL OF SOLAR ENERGY ENGINEERING.

Manuscript received by the ASME Solar Energy Division, Mar. 1, 1991; final revision, July 23, 1991.

turbulent flows or incompressible fluids with the Boussinesq approximation. This code was applied to model single ventilated enclosures with a complex environment. The airflow patterns in the ventilated enclosures under different boundary conditions were demonstrated.

Murakami et al. (1988) reported their study of contaminant transport in a turbulent diffusion field. They examined the cases with supplies located on the ceiling and the exhausts mounted near the floor on one pair of opposite side walls. Four types of single, clean room models were used for analysis: the number of supplies on the ceiling was varied from one to four and six and nine. The concentration distributions for cases with different contaminant source locations were examined.

Horstman (1988) developed a numerical model to predict the two-dimensional velocity distribution, circulation pattern, and airborne contaminant distribution within a ventilated volume for a steady-state condition. The two-dimensional laminar flow was solved in the form of finite difference stream functioning equations and modified Taylor series approximations of the vorticity equations. The model was applied to predict the airflow pattern and contaminant build-up in the passenger cabins of commercial aircraft. The central difference scheme was used for the momentum equation, while the upwind difference scheme was adopted for the contaminant conservation equation to ensure the transport in the proper direction.

Chen et al. (1990a) applied a low Reynolds number $k-\epsilon$ turbulence model to predict the velocity and temperature distributions in an enclosure with natural convection flow. They concluded that for computation of indoor air movement, the low Reynolds number $k-\epsilon$ model provides a better velocity profile in the region near the walls and more accurate simulations of the convective heat transfer from walls to room air than the $k-\epsilon$ model.

In a later work, Chen et al. (1990b) numerically investigated indoor air quality and thermal comfort in a ventilated enclosure for six cases using different kinds of air diffusers. The blockage due to furniture and contaminants emitted from the furniture were simulated. Again, the low Reynolds number $k-\epsilon$ model was employed.

The above-mentioned numerical studies are limited to cases of a single zone. Chang et al. (1982) undertook a finite difference study of natural convection in a two-dimensional square enclosure with a partition mounted either on the ceiling or on the floor. One wall parallel to the partition was kept cold while the opposite was kept hot; the ceiling and the floor were well insulated. The two-dimensional laminar flow cases for the Grashof number region from 10^3 to 10^8 were computed with different combinations of the partition geometry and location. It was found that the maximum heat transfer rate occurred when the partition was set slightly off center of the enclosure, towards the hot wall. This model was not validated.

Kelkar and Patankar (1985) predicted natural convection in partitioned enclosures by numerical simulation. The partitions in their studies were two dimensional. The opening on the partition ran through the whole width of the room; the flow conditions were laminar.

A number of computer codes have been developed for three-dimensional analysis of flow and heat transfer study. Among them, the PHOENIX code is the most widely used. The use of these codes, however, does have limitations. Specifically, users do not have the access to the source code and are unable to compare different algorithms or test different iteration procedures. For research purposes, it may be more convenient to have a code developed by the researchers themselves.

Haghighat et al. (1989, 1990a, 1990b) developed a numerical model to study heat and mass transfer phenomena in three-dimensional two-zone enclosures with turbulent flow. The model was applied to investigate the influence of door height and location on interzone natural convective heat transfer rate; the ventilation effectiveness and thermal comfort parameters in a two-zone enclosure for different arrangement of door opening, ventilation supply and exhaust locations. The effect of infiltration on ventilation air movement in a partitioned enclosure was studied as well (Wang et al., 1990). They found that the flow pattern and contaminant distribution in a downstream zone were quite sensitive to the change of door location.

Jiang et al. (1991) studied the airflow pattern, temperature distribution, and percentage of dissatisfied people in a two-zone enclosure with a mixed convection condition.

The main objectives of this paper are: (1) to describe the development of a numerical model which simulates the interzonal convective heat and mass transfer in three-dimensional turbulent flows for natural, forced, and mixed convection situations for a two-zone enclosure, (2) to describe the test facility which was used to verify the model, and (3) to compare the data from measurement and from prediction.

Nomenclature (cont.)

A = general cell surface area
A = Van driest's constant
A_x, A_y, A_z = cell surface areas in the x, y, and z-direction, respectively
a = neighbor coefficient of finite difference form
b = source term in discretization equation
C = contaminant concentration
C_1, C_2, C_3 = coefficients in $k-\epsilon$ model
C_μ', C_μ, C_D = coefficients in turbulence model
C_p = specific heat at constant pressure
D = diffusion coefficient
D = diffusion transportation at interfaces of control volumes, $\Gamma A_x/\delta x$
E = wall roughness coefficient in wall function
F = convection transportation at the interfaces of control volumes, $\rho u A_x$
g = acceleration due to gravity
G_B = generation of turbulent kinetic energy related to buoyancy
G_k = stress production of turbulent kinetic energy
Gr = Grashof number, $\beta g \Delta T H^3/\nu^2$
H = height of room
H = enthalpy
h = specific enthalpy
h = height of openings
h_x = convective heat-transfer coefficient
I = turbulence intensity
k = kinetic energy of turbulence
L = room length
l_1 = hydraulic diameter of inlet, $2w_I h_I/(w_I + h_I)$
Nu, Nu_H = Nusselt number based on room height $qH/(T_H - T_c)\lambda$
p = pressure
Pe = cell Peclet number, F/D
Pr = Prandtl number ν/α
q = heat flux per unit area
Ra = Rayleigh number based on room height, $g\beta H^3 (T_H - T_C)/\nu\alpha$

Table 1 Source term for conservation equation

ϕ	Γ_ϕ	S_ϕ
1	0	0
u	μ_{eff}	$-\frac{\partial p}{\partial x}+\frac{\partial}{\partial x}\left(\mu_{eff}\frac{\partial u}{\partial x}\right)+\frac{\partial}{\partial y}\left(\mu_{eff}\frac{\partial v}{\partial x}\right)+\frac{\partial}{\partial z}\left(\mu_{eff}\frac{\partial w}{\partial x}\right)$
v	μ_{eff}	$-\frac{\partial p}{\partial y}+\frac{\partial}{\partial x}\left(\mu_{eff}\frac{\partial u}{\partial y}\right)+\frac{\partial}{\partial y}\left(\mu_{eff}\frac{\partial v}{\partial y}\right)+\frac{\partial}{\partial z}\left(\mu_{eff}\frac{\partial w}{\partial y}\right)$
w	μ_{eff}	$-\frac{\partial p}{\partial z}+\frac{\partial}{\partial x}\left(\mu_{eff}\frac{\partial u}{\partial z}\right)+\frac{\partial}{\partial y}\left(\mu_{eff}\frac{\partial v}{\partial z}\right)+\frac{\partial}{\partial z}\left(\mu_{eff}\frac{\partial w}{\partial z}\right)-\rho\beta g\theta$
h	$\frac{\mu_{eff}}{\sigma_h}$	0
k	$\frac{\mu_{eff}}{\sigma_k}$	$G_k-\rho\epsilon+G_B$
ϵ	$\frac{\mu_{eff}}{\sigma_\epsilon}$	$C_1\frac{\epsilon}{k}(G_k+G_B)(1+C_3R_f)-C_2\frac{\rho\epsilon^2}{k}$
c	$\frac{\mu_{eff}}{\sigma_c}$	0

Brief Description of the Concordia Code

Physical Foundation. This model employs the finite difference method and the $k-\epsilon$ two-equation model of turbulence to obtain the approximate solution of the governing equations for the three-dimensional turbulent flow in Cartesian coordinates.

The governing equations can be written in a common form as follows:

$$\frac{\partial\rho\phi}{\partial t}+\frac{\partial}{\partial x_i}(\rho u_i\phi)=\frac{\partial}{\partial x_i}\left(\Gamma_{\phi,\,\mathrm{eff}}\frac{\partial\phi}{\partial x_i}\right)+S_\phi \tag{1}$$

where ϕ denotes the variables u_i, h, c, k, or ϵ. S_ϕ represents the source term for each of the variables listed in Table 1.

Nomenclature (cont.)

Ra_L = Rayleigh number based on room length, $g\beta L^3(T_H-T_C)/\nu\alpha$
Ra^* = flux Rayleigh number, $g\beta qH^4/k\nu\alpha$
Re = Reynolds number, $U_I l_I/\nu$
S_ϕ = source term for variable ϕ
T = temperature
T_c = cold wall temperature
T_H = hot wall temperature
t = time
$u_i(u,v,w)$ = velocity in x, y, z-direction, respectively
U_I = air velocity at ventilation inlet
x,y,z = Cartesian coordinate system
x_D = distance from western wall ($x=0$) to partition
y_D = distance from southern wall ($y=0$) to door axis
w = width of opening
W = width of room

Greek Symbols

Γ_ϕ = exchange coefficient of ϕ
δx = distance between nodes
Δ = difference
Δx, Δ_y, Δz = dimensions of control volume
ϵ = dissipation rate of turbulence energy
κ = von Karman's constant
λ = thermal conductivity
μ = dynamic viscosity
ν = kinematic viscosity
ρ = density
σ = exchange coefficient
σ_t = turbulent Schmidt number or Prandtl number
τ = shear stress
ϕ = dependent variables in conservation equation

Subscripts

c = contaminant
D = door
E = exhaust opening
E,W,N,S,T,B = grid node at east, west, north, south, top, and bottom, respectively
eff = effective
h = door height
I = supply inlet
P = currently considered node
p = grid node adjacent to solid surface
s = source
t = turbulent
ϕ = dependent variables

$\Gamma_{\phi,\,\mathrm{eff}}$ is the effective exchange coefficient. For the momentum equation, it is the sum of eddy viscosity and molecular viscosity:

$$\Gamma_{u,\,\mathrm{eff}}=\mu_{u,\,\mathrm{eff}}=\mu_t+\mu. \tag{2}$$

For other scalars, the effective exchange coefficients can be expressed in terms of the effective viscosity coefficient as

$$\Gamma_{\phi,\,\mathrm{eff}}=\frac{\mu}{\sigma_\phi}+\frac{\mu_t}{\sigma_{\phi,\,t}} \tag{3}$$

where σ_ϕ and $\sigma_{\phi,\,t}$ are the laminar and turbulent exchange coefficient ratios, respectively. They are referred to the laminar and the turbulent Prandtl number or Schmidt number. Their values are usually obtained from experimental data.

In the $k-\epsilon$ two-equation model, the turbulent viscosity is determined by

$$\nu_t=C_\mu\frac{k^2}{\epsilon}. \tag{4}$$

The numerical values of the coefficients appearing in the source terms for k and ϵ are all determined from experiments. At high Reynolds numbers they are approximately constant. In the present study the following values, recommended by Launder and Spalding [27], are assigned to the constants:

$$C_1=1.44 \quad C_2=1.93 \quad C_\mu=0.09 \quad C_D=1.0$$

$$\sigma_K=1.0 \quad \sigma_\epsilon=1.3 \quad \sigma_t=1.0.$$

Wall Function Method. In the region near solid surfaces, the gradients of flow property variation are high, and the turbulent viscosity is no longer dominant. The $k-\epsilon$ model, which is applicable only for high Reynolds number turbulent flows, is not valid in this region and a special treatment is required to describe the flow properties. The wall function method is the most widely used to deal with this problem.

The wall functions are based on the one-dimensional steady-state boundary layer equations and the mixing-length hypothesis. The principle of the wall function method is to modify the source terms in the conservation equations for the grid nodes near the solid surfaces by using the momentum flux due to shear stress and the heat flux at solid surfaces.

The wall function employed here is

$$u^+=\frac{\ln(EY^+)}{\kappa} \tag{5}$$

and

$$T^+=\sigma_t(u^++P) \tag{6}$$

where k is von Karman's constant ($k=0.435$). E is a coefficient reflecting the roughness of the walls. For smooth walls, E can be theoretically determined as 9.0 (Whittle, 1986). P can be either deduced directly from experimental data or evaluated theoretically based on the Van Driest hypothesis, which results in (Launder and Spalding, 1972):

$$P=\frac{\pi}{4\sin(\pi/4)}\left(\frac{A}{\kappa}\right)^{1/2}\left(\frac{\sigma_h}{\sigma_{h,\,t}}-1\right)\left(\frac{\sigma_{h,\,t}}{\sigma_h}\right)^{1/4}. \tag{7}$$

The fluxes of momentum and heat to solid surfaces are then determined by Eqs. (5) and (6). They can be written as (Launder and Spalding, 1972):

$$\frac{u_p}{\tau_s/\rho}C_\mu^{1/4}k_p^{1/2}=\frac{1}{\kappa}\ln\left[EY_p\frac{(C_\mu^{1/2}k_p)^{1/2}}{\nu}\right] \tag{8}$$

$$\frac{(T_p-T_s)C_{p\rho}C_\mu^{1/4}k_p^{1/2}}{q_s}=\frac{\sigma_{h,\,t}}{\kappa}\ln\left[Ey_p\frac{(C_\mu^{1/2}k_p)^{1/2}}{\nu}\right]$$

$$+\sigma_{h,\,t}\frac{\pi}{4\sin(\pi/4)}\left(\frac{A}{\kappa}\right)^{1/2}\left(\frac{\sigma_h}{\sigma_{h,\,t}}-1\right)\left(\frac{\sigma_{h,\,t}}{\sigma_h}\right)^{1/4}. \tag{9}$$

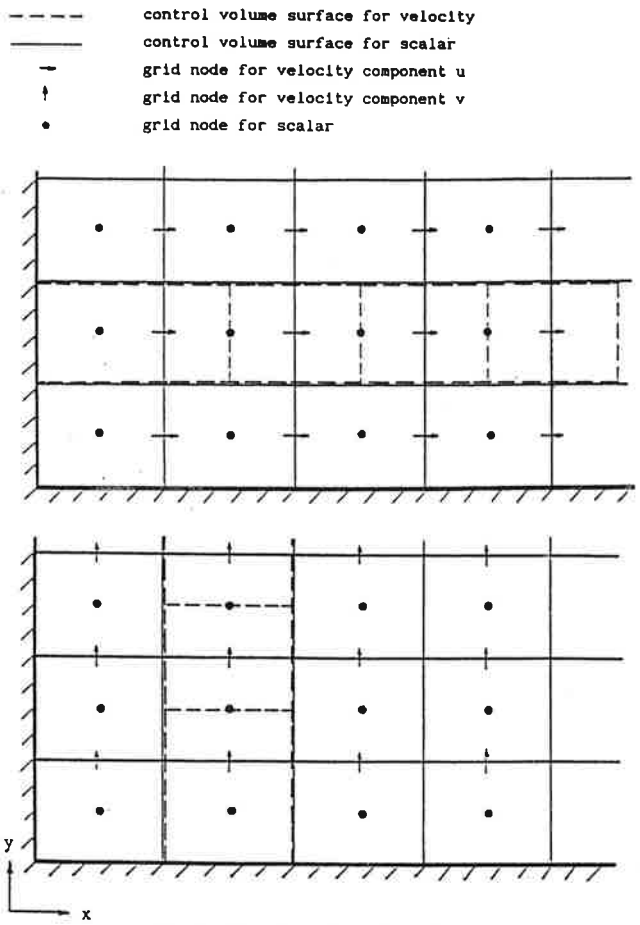

Fig. 1 Structure of mesh system

However, when the wall function method is applied, the grid nodes near walls must be sufficiently remote from walls to ensure that the turbulent Reynolds number, $(k^{1/2}1/\nu)_p$, is much greater than unity, and that the viscous effects are entirely overwhelmed by those of turbulent viscosity.

Numerical Procedure

Finite Domain Equations. A three-dimensional mesh system in Cartesian coordinates is employed in the model with the staggered control volumes for velocity components in the X, Y, Z-directions, as shown in Fig. 1.

In each of the control volumes, the variables are assumed to have a uniform value. Consequently, integrations can be performed over each control volume to yield the discretization equations expressed as:

$$\phi_p=\frac{a_w\phi_w+a_E\phi_E+a_N\phi_N+a_S\phi_S+a_T\phi_T+a_B\phi_B+b}{a_p} \tag{10}$$

with

$$b=S_c\Delta x\Delta y\Delta Z+a_p^o\phi_p^o \tag{11}$$

$$a_p=a_W+a_E+a_N+a_S+a_T+a_B+a_p^o-S_p\Delta X\Delta Y\Delta Z \tag{12}$$

$$a_p^o=\rho_p^o\frac{\Delta x\Delta y\Delta z}{\Delta t} \tag{13}$$

where a is the neighbor coefficient determined by the interpolation profile in difference scheme and the superscript "o" indicates the value in the last time step. The hybrid scheme developed by Spalding (1972) is adopted, which is a combination of the central difference scheme and the upwind scheme but neglecting the diffusion term in the upwind scheme. The switch between the two schemes is controlled by the cell Peclet

number, which denotes the strength ratio of convection to diffusion defined as

$$P_e = \frac{\rho u(\Delta x)}{\Gamma}. \tag{14}$$

For each variable, there is an algebraic equation like Eq. (10) in each of the control volumes. The solution for these algebraic equations can be obtained by solving a triangular matrix with line-by-line iteration procedure.

The SIMPLE algorithm is employed to solve the finite difference equations (Patankar and Spalding, 1972). The alternating directional implicit (ADI) method, and the false time step with underrelaxation are also employed in the iteration procedure. Details of these procedures are well documented in the literature (i.e., Patankar, 1980).

In order to ensure the mass continuity at the door opening where the flow properties may change rapidly, an overall correction on the velocity component in the direction perpendicular to the partition (the x-direction) is added for each vertical section parallel to the partition. At the door opening, the overall correction serves as an outflow boundary condition for the upstream zone and an inflow boundary condition for downstream zone. The necessity of the overall continuity correction is caused by the accumulated error in each iteration process. The overall correction term, derived from the mass continuity over the sections parallel to the partition, can be expressed as:

$$\Delta u = \frac{Q_{up} - Q}{\Sigma A_{x,j}} \tag{15}$$

where Q represents the air volume flow rate across the section before velocity is overall corrected. The summation is carried out over the whole section perpendicular to the x-direction.

Grid Dependence Tests (Sensitivity Analysis). The accuracy of computation results is affected by the number of grid nodes to a certain extent. However, computation cost requires that the grid number be minimized. The aim of grid dependence test is to select a mesh system with the smallest possible grid number and satisfactory accuracy. In the grid-dependence test, computations are carried out with an increasing number of grid node until the further increment shows negligible change in solution.

In a grid-dependence test, the velocity components in three directions at the center of the enclosure are computed with the following five mesh systems. They are: $8\times8\times14$, $10\times10\times16$, $12\times12\times18$, $14\times14\times20$, and $24\times24\times36$. The magnitudes of the velocity component in the x-direction at the center of the door opening obtained from the five mesh systems and the relative variations are:

mesh system	$8\times8\times14$	$10\times10\times16$	$12\times12\times18$	$14\times14\times20$	$24\times24\times36$
U	1.55E-2	1.62E-2	1.66E-2	1.69E-2	1.72E-2
difference		4.5%	2.5%	1.8%	1.7%

The grid dependence test indicates that, for the sake of economy, the accuracy with a $10\times10\times16$ system may be acceptable for an enclosure with $L\times W\times H = 10\text{m} \times 4\text{m} \times 3\text{m}$ for natural convection. However, in forced and mixed convection studies, a finer mesh system is required to simulate ventilation supply, exhaust, and contaminant source.

Convergence of the iteration process is pronounced when the total absolute value of residual sources in the continuity equation with starred velocity field is small enough (less than one percent relative error) and when the variation in value of variable between two iteration is small enough (less than 0.01 percent relative error). The reason for choosing the residual source in continuity equation as a monitor is that the convergence of continuity equation in this study is slower than the other variable.

Validation of the Numerical Model

Validation of the numerical model was performed by comparing the predicted results in natural convection with experimental data obtained by Nansteel and Greif (1984) and by the results of a specially designed experiment (Allard et al., 1987), while for forced convection, a comparison with the PHOENICS code was carried out.

Comparison With Experimental Data Obtained by Nansteel and Grief. The Nusselt number, as a function of Rayleigh number, from computation and from the measurements reported by Nansteel and Grief (1984) are shown in Fig. 2.

The thermal boundary conditions used in the computation are the same as those in the experiment. Since the cell size is restricted by the number of grids, the parameter w_D/W, which is 0.25 in numerical calculation, does not match the value 0.093 adopted in the experiment. However, in the experiment it was found that the door width had little influence on the interzone heat convection rate. For example, the interzone convective heat transfer rate for the case with $w_D/W = 1$ was only five percent higher than that with $w_D/W = 0.093$ when the door height is three quarters of the room height.

Figure 2 shows that in the relatively high Rayleigh number region ($\text{Ra}_L > 3*10^{11}$), the computed Nusselt number is slightly higher than the projection of the correlation line obtained by Nansteel and Grief and slightly lower than the experimental data obtained by Weber (1980). In the region of $\text{Ra}_L < 3*10^{11}$, the predicted Nusselt number is slightly lower than the experimental data obtained by Nansteel and Grief. The $k-\epsilon$ model combined with the wall function method, although applicable in the region that the experiment covers, may not give good predictions of heat flux from walls when the Rayleigh number is relatively low. The low Reynolds number $k-\epsilon$ model of turbulence would be more suitable to predict the natural convection phenomena in buildings.

In general, the agreement is satisfactory between computed values of Nu and the experimental data (Patankar, 1980; Allard et al., 1987).

Comparison With Experimental Data. A specially designed experiment was set up to measure air velocity and temperature distribution in a two-zone enclosure, (Allard, 1987). The two-zone enclosure had a dimension of $L\times W\times H$ = 6.3 m × 3.1 m × 2.5 m, Fig. 3. A partition was placed at the middle of the room length with a centrally located door opening (1.85 m height and 0.77 m width). There was a step of 0.08 m height at the door opening. The thickness of the partition was 0.07 m. The velocity and temperature fields through the doorway were measured by a hot film probe and a 0.08-mm diameter thermocouple. An automatic displacement system was used to move these two probes in the central plane of the doorway.

The isothermal boundary conditions for the walls, ceiling, and floor were:

$$T_W = 11.70°\text{C} \quad T_E = 17.93°\text{C}$$
$$T_N = 17.32°\text{C} \quad T_S = 17.20°\text{C}$$
$$T_T = 17.10°\text{C} \quad T_B = 16.71°\text{C}.$$

Figure 4 shows the velocity distribution at the center of the door opening obtained by experimental measurement and numerical computation. Discrepancy is observed in the low region of the door opening. It might be caused by the 0.08-m step on the floor of the door opening which is neglected in the

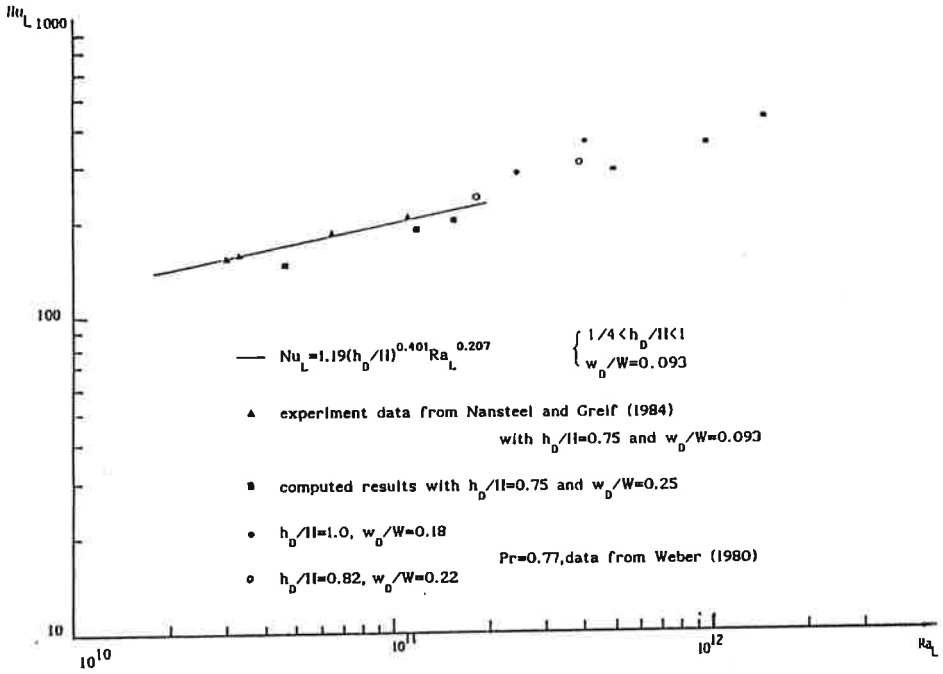

Fig. 2 Comparison with experimental measurements

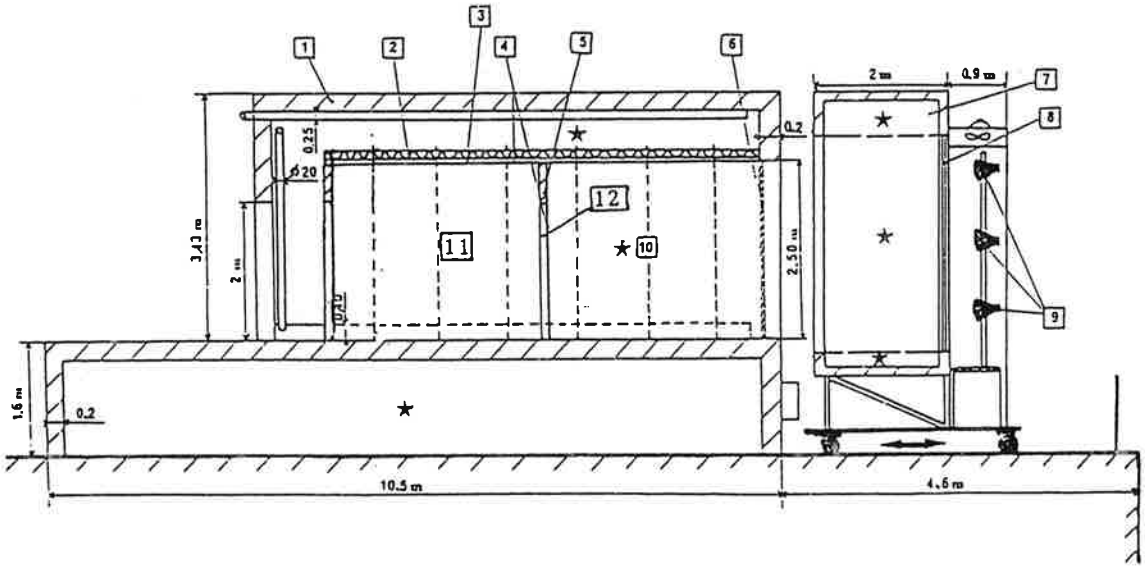

Nomenclature :

1 : external envelope (cellular concrete e=20 cm)
2 : fibreglass (e=5cm)
3 : plywood (e=2,5cm)
4 : gypsum board (e=1cm)
5 : fibreboard (e=5cm)
6 : glazing (e=1cm)
7 : mobile climatic housing
8 : double glazing (10-8-10 mm)
9 : solar simulator (12 lamps CSI 1000 W)
10 : test cell 1
11 : test cell 2
12 : doorway

Fig. 3 Longitudinal section of the minibat cell

computation since it is too small to be considered in the uniform mesh system adopted. In the left part of the door opening, the predicted velocity distribution is in very good agreement with the experimental data.

The temperature distribution at the center of the door opening plane is presented in Fig. 5. The computed temperatures at the middle region of the door height is lower than the measurement by more than one degree. At higher and lower

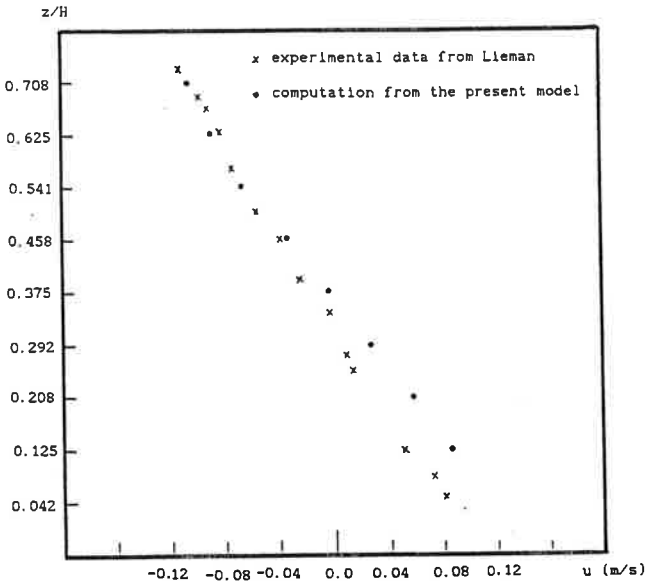

Fig. 4 Velocity distribution at the center of the door opening in comparison with measurements

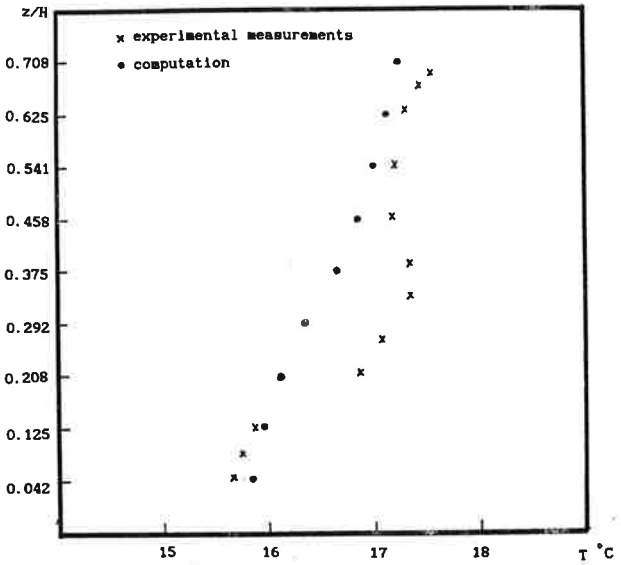

Fig. 5 Temperature distribution at the center of the door opening

regions the agreement between computation and measurements is satisfactory.

Comparison With Results Predicted by the PHOENICS Code. The configuration used in computation for comparison is presented in Fig. 6. A partition is fixed at the middle of the enclosure dividing it into two equal-sized zones. A ventilation supply opening is located on the western wall in zone A, and an exhaust opening is mounted on the ceiling in zone B. Table 2 lists the dimensions and the locations of the openings of the door, supply, and exhaust. A contaminant source is place in the central area of zone A. The air velocity at the supply opening is 0.1 m/s which provides a ventilation rate of 2.5 each. The k and ϵ at the supply opening is

$$k_{in} = 1.5(0.1\ U_{in})^2$$

$$\text{and } \epsilon_{in} = \frac{C_\mu (k_{in})^{1.5}}{l}. \tag{6}$$

l is a characteristic length determined by the opening size and geometry. At the exhaust opening, the air velocity can be determined by the overall mass balance, while other variables have zero gradient in the direction perpendicular to the opening plane.

The ceiling, floor, and walls are considered to be well in-

Table 2 The dimensions and locations of the opening

	door	supply	exhaust
dimension w/W	0.17	0.083	0.083
h/H	0.75	0.083	---
l/L	---	---	0.056
location x/L	0.5	0.0	0.75
y/W	0.83	0.13	0.875
z/H	---	0.042	1.0

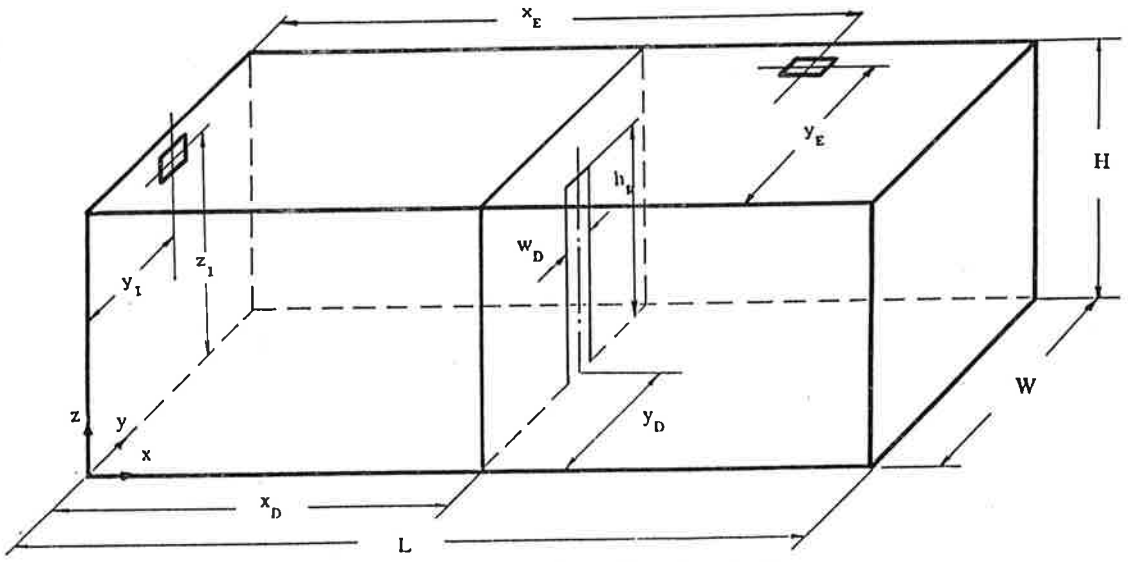

Fig. 6 Configuration of a partitioned enclosure

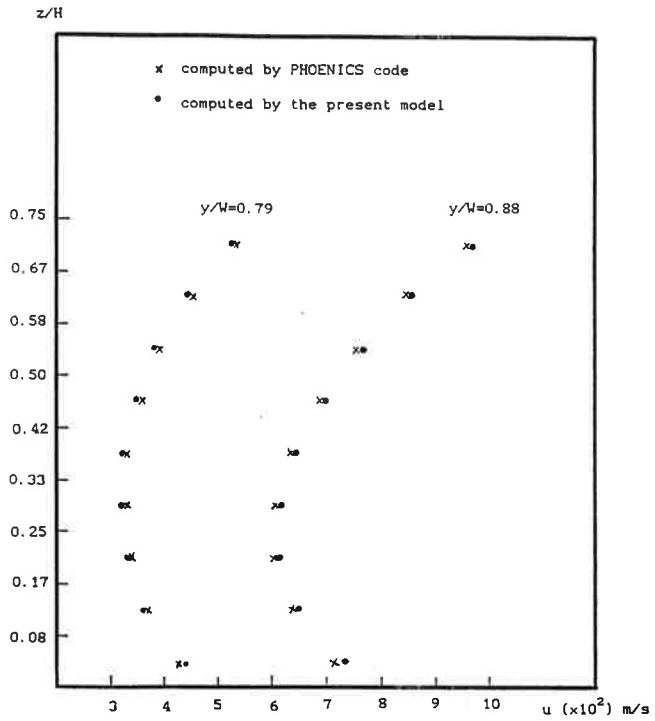

Fig. 7 Velocity distributions at the door opening ($x/L = 0.5$) in comparison with the PHOENICS code

sulated, therefore an isothermal airflow could be assumed. The thickness of the partition is negligibly small in comparison with the length of the enclosure. Besides, it is assumed that the contaminant is emitted from a point source, and its emission rate is negligibly small in comparison with the ventilation flow rate.

The velocity distributions at the door opening predicted by the Concordia code and the PHOENICS code are presented in Fig. 7. It is seen that the agreement of both velocity distribution and average contaminate concentration in each zone, computed by the Concordia code and the PHOENICS code, is very good.

Parametric Studies

The numerical model was applied to parametric studies for an enclosure with two zones connected by a doorway. The effects of the door size and location on interzone convective heat and mass transfer were examined. It was found, in a natural convection case, that the door height has a strong impact on heat convection from the hot zone to the cold zone, while moving the door opening from the middle of the partition toward a side wall increases the convective heat transfer slightly (Haghighat et al., 1989). When the enclosure is ventilated by the mechanical system with the supply and exhaust openings being in different zones, the computed results show that the location of the supply opening has a significant effect on indoor air motion while the influence of the exhaust opening is less, and that the airflow pattern and contaminant distribution in the downstream zone are more sensitive to the door location than the upstream zone (Haghighat et al., 1990a).

Conclusion

Computational fluid dynamics is a powerful tool for the study of indoor environment and has been used by many researchers. However, the majority of the previous numerical investigations have focused on single-zone configurations. The simulation of multizone environments is generally based on the assumption of uniform distributions of air velocity, temperature, and contaminant concentration in each zone. This type of modeling is inadequate for advanced investigations of indoor air quality and thermal comfort, and more precise analyses are required.

Table 3 Locations of openings for basic model in ventilation effectiveness study

	door	supply	exhaust	source
x/L	0.5	0.0	0.75	0.25
y/W	0.5	0.46	0.875	0.46
z/H	-	0.875	1.0	0.46

A numerical model was developed and applied to analyze indoor air movement and accompanying heat and mass transfer in three-dimensional, two-zone enclosures with turbulent flow. This model was used to predict the field distributions of parameters affecting indoor air quality and thermal comfort such as velocity, temperature, contaminant concentration, and turbulence intensity. The validation of the model was carried out by comparing the predicted results with available experimental data. The results obtained show that proper location of supply, exhaust, and door openings can be important in attempting to improve indoor air quality in each zone.

Acknowledgments

This study was financially supported by the Natural Sciences and Engineering Research Council of Canada, and "Fonds pour la Formation de Chercheurs et l'Aide a la Recherche."

References

Allard, R., Brau, C., Inard, C., and Pallier, J. M., 1987, "Thermal Experiments of Full Scale Dwelling Cells in Artificial Climatic Conditions," *Energy and Buildings*, Vol. 10, pp. 49–58.

Berne, P., and Villand, M., 1987, "Prediction of Air Movement in a Ventilated Enclosure with 3-D Thermohydraulic Code TRIO," *ROOMVENT-87*, Vol. 3, Stockholm, pp. 1–15.

Catton, I., 1978, "Natural Convection in Enclosures," *Heat Transfer*, Vol. 6.

Chang, L. C., Lloyd, J. R., and Yang, K. T., 1982, "A Finite Difference Study of Natural Convection in Complex Enclosures," *Proceedings of the 7th International Heat Transfer Conference*, Vol. 2, pp. 183–188.

Chen, Q., Moser, A., and Huber, A., 1990, "Prediction of Buoyant, Turbulent Flow by a Low-Reynolds-Number $k-\epsilon$ Model," *ASHRAE Transactions*, Vol. 96, Pt. 1, pp. 564–573.

Chen, Q., Moser, A., and Suter, P., 1990, "Indoor Air Quality and Thermal Comfort Under Six Kinds of Air Diffusion," presented at ASHRAE Winter Meeting.

Chen, Q., and Van der Kooi, J., 1988, "ACCURACY—A Program for Combined Problems of Energy Analysis, Indoor Airflow, and Air Quality," *ASHRAE Transactions*, Vol. 94, Pt. 2, pp. 196–214.

Gadgil, A., Bauman, F., Altmayer, E., and Kammerund, R. C., 1984, "Verification of a Natural Simulation Technique for Natural Convection," ASME Journal of Solar Energy Engineering, Vol. 106, pp. 366–369.

Hadjisophocleous, G. V., Sousa, A. C. M., and Venart, J. E. S., 1988, "Prediction of Transient Natural Convection in Enclosures of Arbitrary Geometry Using a Nonorthogonal Numerical Model," *Numerical Heat Transfer*, Vol. 13, p. 373.

Haghighat, F., Jiang, Z., and Wang, J. C. Y., 1989, "Natural Convection and Airflow Pattern in a Partitioned Room With Turbulent Flow," *ASHRAE Transactions*, Vol. 95, Pt. 2, pp. 600–610.

Haghighat, F., Wang, J. C. Y., and Jiang, Z., 1990a, "Three Dimensional Analysis of Airflow Pattern and Contaminant Dispersion in a Ventilated Two-Zone Enclosure," *ASHRAE Transactions*, Vol. 96, Part 1, pp. 831–939.

Haghighat, F., Wang, J. C. Y., and Jiang, Z., 1990b, "Development of a Three-Dimensional Numerical Model to Investigate the Airflow and Age Distribution in a Multizone Enclosure," *Proceedings of the 5th International Conference on Indoor Air Quality and Climate: Indoor Air'90*, Vol. 4, Toronto, Canada, pp. 183–188.

Holmes, M. J., 1982, *The Application of Fluid Mechanics Simulation Program PHOENICS to a Few Typical HVAC Problems*, Ove Arup and Partners, London.

Horstman, R. H., 1988, "Predicting Velocity and Contamination Distribution in Ventilated Volumes Using Navier-Stokes Equations," *Proceedings of the ASHRAE Conference*, IAQ 88, Atlanta, GA, Apr. 11–13, 1988, pp. 209–230.

Jiang, Z., Hghighat, F., and Wang, J. C. Y., 1991, "Thermal Comfort and Indoor Air Quality in a Partitioned Enclosure Under Mixed Convection," *Building and Environment*, accepted for publication.

Jones, P., and Sulivan, P. O., 1985, "Modelling of Air Flow Patterns in Large Single Volume Space," SERC Workshop: Development in Building Simulation Programs, Loughborough University.

Kelkar, K. M., and Patankar, S. V., 1985, "Numerical Prediction of Natural Convection in Partitioned Enclosures," *Numerical Heat Transfer*, pp. 63-71.

Launder, B. E., and Spalding, D. B., 1972, *Mathematical Model of Turbulence*, Academic Press.

Lemaire, A. D., 1987, "The Numerical Simulation of the Air Movement and Heat Transfer in a Heated Room Resp. A Ventilated Atrium," *Proceedings of the International Conference on Air Distribution in Ventilated Space, ROOMVENT-87*, Stockholm.

Lin, D. S., and Nansteel, N. W., 1987, "Natural Convection Heat Transfer in a Square Enclosure Containing Water Near Its Density Maximum," *International Journal of Heat and Mass Transfer*, Vol. 30, No. 11, pp. 2319-2329.

Markatos, N. C., 1983, "The Computer Analysis of Building Ventilation and Heating Problems," *Passive and Low Energy Architecture*, pp. 667-675.

Markatos, N. C., and Pericleous, K. A., 1984, "Laminar and Turbulent Natural Convection in an Enclosed Cavity," *International Journal of Heat and Mass Transfer*, Vol. 27, No. 5, pp. 755-772.

Murakami, S., Kota, S., and Suyama, Y., 1988, "Numerical and Experimental Study on Turbulent Diffusion Fields in Convectional Flow Type Clean Rooms," *ASHRAE Transactions*, Vol. 94, Pt. 2, pp. 469-493.

Nasteel, M. W., and Grief, R., 1984, "An Investigation of Natural Convection in Enclosures with Two and Three Dimensional Partitions," *International Journal of Heat and Mass Transfer*, Vol. 27, No. 4, pp. 561-571.

Ostrach, S., 1982, "Natural Convection Heat Transfer in Cavities and Cells," *Proceedings of the International Heat Transfer Conference*, Hemisphere, Washington, D.C., pp. 365-379.

Patankar, S. V., 1980, *Numerical Heat Transfer and Fluid Flow*, Hemisphere, New York.

Patankar, S. V., and Spalding, D. B., 1972, "A Calculation Procedure for Heat, Mass, and Momentum Transfer in Three-Dimensional Parabolic Flows," *International Journal of Heat and Mass Transfer*, Vol. 15, p. 1787.

Pun, W. M., and Spalding, D. B., 1976, "A General Computer Program for Two-Dimensional Elliptic Flows," HTS/76/2, Imperial College, London.

Spalding, D. B., 1972, "A Novel Finite-Difference Formulation for Differential Expression Involving Both First and Second Derivatives," *Internal Journal of Numerical Methods in Engineering*, Vol. 4, p. 551.

Wang, J. C. Y., Jiang, Z., and Haghighat, F., 1990, "Influence of Air Infiltration on Isothermal Airflow and Contaminant Field in a Partitioned Enclosure," *Energy and Buildings*, Vol. 17, pp. 43-54.

Weber, D. D., 1980, "Simulation Modeling of Natural Convection Heat Transfer Through an Aperature in Passive Solar Heated Building," Ph.D. Thesis, Department of Physics, University of Idaho, Moscow, Idaho.

Whittle, G. E., 1986, "Computation of Air Movement and Convective Heat Transfer Within Buildings," *International Journal of Ambient Energy*, Vol. 7, No. 3, pp. 151-165.